Tip size effect on the appearance of a STM image for complex surfaces: Theory versus experiment for Si(111)-(7×7)

Y. L. Wang, H.-J. Gao, H. M. Guo, and H. W. Liu
Institute of Physics, Chinese Academy of Sciences, Beijing 100080, China

I. G. Batyrev, W. E. McMahon, and S. B. Zhang
National Renewable Energy Laboratory, Golden, Colorado 80401, USA
(Received 4 May 2004; published 30 August 2004)

Scanning tunneling microscopy experiment and first-principles total energy calculation are combined to determine STM images for Si(111)-7×7 to resolve the long-time discrepancy between theory and experiment. Our experiment resolves clearly and simultaneously the rest and adatom spots, in good agreement with theory, with the rest atom spots almost as bright as those of the central adatoms in the unfaulted-half of the unit cells. Theoretical study suggests that a geometric hindrance effect due to finite tip size could be responsible for the past experimental inability to observe the rest atoms.

DOI: 10.1103/PhysRevB.70.073312 PACS number(s): 68.37.Ef, 68.35.−p, 73.20.−r

The invention of scanning tunneling microscopy (STM)[1] and the determination of the Si(111)-7×7 atomic reconstruction[2] are two of the single most important events in the history of surface science and technology. It is therefore not surprising that one of the first systems tested by the STM is the reconstruction of the 7×7 surface,[3] revealing twelve bright spots corresponding to the adatoms. It is now understood that the STM probes the real-space charge distribution near the Fermi level (E_F) in a rather delicate way that may or may not reveal the *unperturbed* real-space charge distribution of the surfaces.[4] For example, for the Si(111)-7×7 surface, state-of-the-art first-principles electronic structure calculations show a strong dependence of the charge distribution (or the so-called theoretical STM image) on the bias voltage V_{bias}: twelve spots at $V_{bias}=-0.57$ V for the twelve adatoms [half of them are brighter than the other, see Fig. 1(a)], whereas eighteen spots at $V_{bias}=-1.5$ V for the twelve adatoms plus six rest atoms [see Fig. 1(b)]. For over 20 years, despite countless studies of the Si(111)−7×7 surface, however, no one has produced STM images to clearly account for the calculated charge distributions.

Regardless, to a large extent, of the bias applied, the experimental STM images reveal only twelve adatom spots.[5–10] The rest atom spots are seen, but only by special techniques[7,11] at a price of suppressing the adatom spots. This inability has led to the perception that the measured tunneling current for semiconductors consists mostly of states near the Fermi level instead of the states further away, due to the exponential dependence of the tunneling probability on the energy level position.[6] Since the adatom dangling bond states are about 0.4 eV below the E_F, whereas those of the rest atoms are about 0.8 eV below,[7] standard STM images are always "distorted" to reveal only the former but not the latter.

In this paper, we show that the calculated voltage-dependent charge distributions of the Si(111)-7×7 surface, thus the "ultimate" STM images, can be reasonably well reproduced by the STM experiments. This is significant because by bringing agreement between first-principles calculations and experiments after twenty years, a *perceived* fundamental limitation blocking direct comparison between theoretical and experimental STM images has been removed. A careful preparation of the STM tips, reducing the radius of the apex to near or less than 1 nm, may have been the key to the success, as our first-principles calculations reveal a geometric hindrance effect of the apex for such complex surfaces. More generally, it is known that the STM image for complex molecules on a surface can be significantly different from the known structures, e.g., the imaged lateral dimension of a cylindrical carbon nanotube can be a few times larger than its height.[12] In an AFM experiment, due to the relatively large tip-size, the lateral dimension of a spherical quantum dot can also be order of magnitude larger than the height.[13] Hence, the implication of the current study could go well beyond just the Si(111)-7×7 reconstruction.

We carried out the calculation by using first-principles density function theory,[14] as implemented in the VASP codes.[15] The Vanderbilt ultrasoft pseudopotential[16] was used with a cutoff energy equal to 170 eV and 1 special *k*-point in the Brillouin zone sum. The surface unit cell contains a slab of six Si layers (without counting the Si adatoms) and a vacuum layer equivalent to six Si layers. The front surface contains the 7×7 reconstruction in the Takayanagi model,[2] whereas the back surface is hydrogen-passivated. Except for the very bottom layer, all of the Si atoms were fully relaxed to minimize the system total energy.

Figure 2 shows the calculated atomic structure of the 7×7 surface. The rhomboid unit cell has two halves, one of which has a stacking fault in the second layer. Thus, they are termed faulted and unfaulted halves. The topmost Si layer has twelve adatoms per unit cell, evenly distributed between the faulted and unfaulted halves. In the second Si layer, there exist six Si rest atoms. These are surface atoms that have not been covered by the Si adatoms. Counting also the Si atom inside the corner hole, each 7×7 cell contains $12+6+1=19$ dangling bonds pointing to the vacuum. It is generally accepted that the tunneling current in the standard STM measurements originates from these dangling bonds.

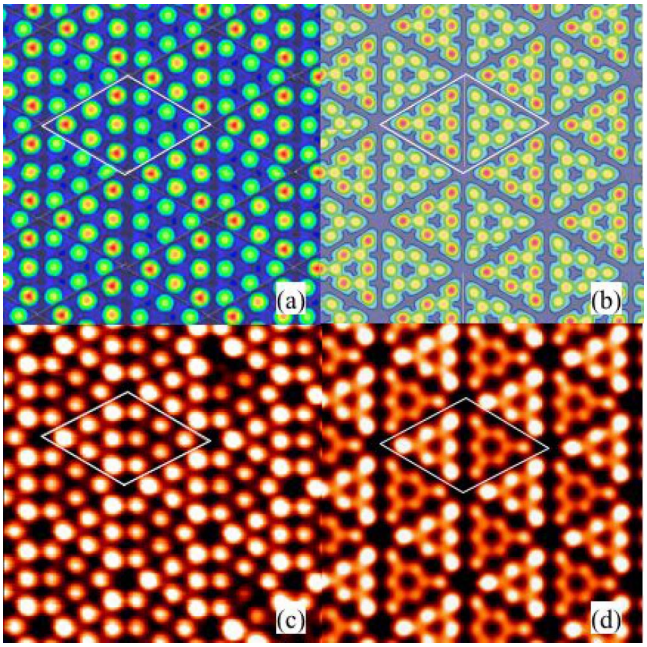

FIG. 1. (Color online) (a), (b) Calculated STM images for Si(111)-7×7 with bias voltage$=-0.57$ and -1.5 V, respectively. The red peaks are about 2 Å above the dark blue borderlines. The dark greys are areas without spatial resolution. (c), (d) The experimental STM images with bias voltage$=-0.57$ and -1.5 V, and tunneling current$=0.3$ and 0.41 nA, respectively. The brighter triangles are the faulted halves of the 7×7 unit cells.

Experiments were performed using an ultrahigh-vacuum STM system[17,18] with a base pressure of $\sim5\times10^{-11}$ mbar. The sample was an antimony-doped *n*-type Si(111) wafer (resistance $\rho\approx0.03\ \Omega$ cm, thickness ≈0.5 mm). Before being introduced into the vacuum chamber, the sample was cleaned by ethanol in an ultrasonic bath and rinsed thoroughly by de-ionized water. It was degassed in the ultrahigh vacuum chamber for several hours at about 600 °C. Approximately 1 h before the measurements, the sample was annealed by direct current heating while keeping the pressure below 10^{-10} mbar. The annealing cycle consisted of flashing the sample to 1200 °C for 20 s, rapidly lowering the temperature to about 900 °C, and then slowly decreasing the temperature at a pace of 1–2 °C/s to room temperature. A nearly perfect 7×7 reconstruction was obtained by this method. Sharp STM tips made of polycrystalline tungsten wire with 0.18 mm diameter were etched electrochemically in 2M NaOH and subsequently cleaned in ethanol and distilled water. Out of the many tips which have been produced, however, only two have been able to produce, and produce repeatedly, the eighteen-spot STM images in Fig. 1(c) while the others produce only the standard twelve-spot images.

Figure 1(c) shows the STM image of the Si(111) 7×7 surface at a sample bias $V_{\text{bias}}=-0.57$ V. There appears to be a significant contrast between the faulted and unfaulted halves of the unit cell. With a negative sample bias this low, the electronic states of the rest atoms are outside the range of the bias. Thus, the STM topography here reveals only the twelve topmost adatoms. The adatoms in the faulted half of the unit cell appear noticeably brighter than those in the unfaulted half. In each half, the adatoms at the corners appear also slightly brighter than those near the center. These qualitative features are in good agreement with the calculated real-space charge distribution at this particular bias, shown in Fig. 1(a). The calculated atomic heights of the adatoms, with respect to the adatoms near the center of the unfaulted half, are 0.12 (faulted; corner), 0.08 (faulted; center), 0.01 Å (unfaulted: corner), respectively. Thus, they might account for the observed differences in the adatom appearances, although the differences in the local electronic structures may also play a role.

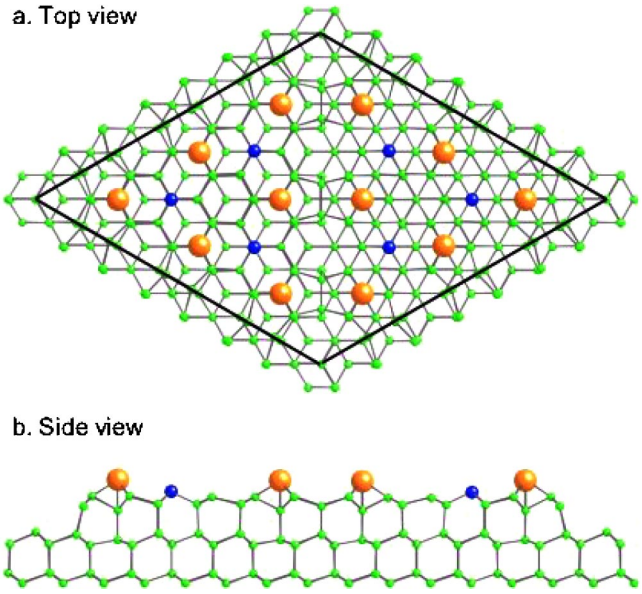

FIG. 2. (Color online) The calculated atomic structures for the Si(111)-(7×7) surface with the faulted half on the left: (a) top and (b) side views. The (large, light) red balls are the Si adatoms whereas the (small, dark) blue balls are the Si rest atoms.

Figure 1(d) shows the STM image at a sample bias $=-1.5$ V. Images of similar quality can be repeatedly reproduced over large areas, e.g., 30×30 nm^2 (not shown). We see clearly in Fig. 1(d) both the adatoms and the rest atoms. On the unfaulted half unit cell, the rest atoms appear to have almost the same brightness as the central adatoms, whereas on the faulted half unit cell, the rest atoms appear to have considerably less brightness than the central adatoms. These observations are again in good agreement with the calculated real-space charge distribution at the experimental bias in Fig. 1(b). The calculated atomic height for the rest atoms, with respect to the adatoms near the center of the unfaulted half, is -0.73 Å and is the same for both the faulted and unfaulted halves. The fact that the rest atoms in the unfaulted half have a similar brightness to the adatoms, which are much closer to the tip, suggests that the dangling bond states of the rest atoms are more extended to the vacuum than the adatoms. This is quite reasonable because, strictly speaking, an adatom is fourfold- instead of threefold-coordinated with the closest neighboring Si atom directly beneath it. This is an example how even subtle differences between the adatoms and the rest atoms in the calculations in Figs. 1(a) and 1(b) can be very well reflected in the experiments in Figs. 1(c) and 1(d).

The experimental results presented here are in sharp contrast to previous STM studies, which in most cases showed images similar to Fig. 1(c) for the Si(111)-7×7 surfaces, irrespective of the bias voltages (somewhere between −2 and 2 V). A common explanation[6] for the absence of the rest atom spots in the images relies on the fact that the tunneling probability depends both on the height and on the thickness of the tunneling barrier. The thickness, in turn, depends approximately linearly on the energy of the tunneling state: the lower the energy is, the thicker the barrier is. Because the tunneling current is inversely proportional to the exponential of the thickness, the lower the state lies in the valence band, the smaller is the tunneling current. Thus, the rest atoms are invisible but the adatoms are visible because the former have significant lower energies than the latter. This argument, however, contradicts our theoretical prediction that the dangling bond states of the rest atoms should extend further into the vacuum region than those of the adatoms. Also, because the rest atoms are approximately $\sqrt{4.5^2+0.73^2}=4.6$ Å away from the nearest adatoms, if one has an infinitely sharp tip positioned right above the rest atom, there is no reason to believe that the adatoms should have any measurable effect on the rest-atom tunneling. If the tunneling current from the rest atom were indeed weak, nothing more would be needed in a constant current STM mode than to move the tip closer to the surface. Hence, this explanation is probably questionable.

Another possible explanation concerns tip contamination by the surface: in other words, a few silicon atoms could be accidentally picked up by the apex of the tungsten tip during the operation, resulting in a semiconducting tip instead of a metallic tip. Indeed, recently it has been shown that an InAs semiconductor tip[11] could be used to enhance rest-atom visibility by utilizing the second gap above the fundamental gap (both lie in the Brillouin zone center) to suppress tunneling current from the high-lying adatom states. However, this is also unlikely in the present case unless the thickness of the contaminant layer exceeds the effective screening length of Si. A previous study[19] showed that the local electronic structure of a typical metal/semiconductor interface remains metallic until several monolayers into the semiconductor.

At this stage, it is impractical for us to determine experimentally what might have happened to the few tips that worked so remarkably well. Instead, here we search for a plausible explanation using first-principles calculations. We noticed that the adatom spots in the calculated STM images, for example, in Fig. 1(a), are often smaller than those in the experimental images. This could be easily explained if the tip has a finite size that reduces spatial resolution. Given the non-flat nature and complexity of the 7×7 reconstruction, such a tip size effect should definitely be examined. Apparently, the actual tip morphology is also complex, possibly with additional atoms adsorbed at the end of the apex (as shown in the inset in Fig. 3). Here, for simplicity, we consider only two simple cases: (a) an apex without any adsorbates, in which we focus our attention on how a relatively large-radius apex could interfere with the STM images, and (b) a cluster of the adsorbates without the apex. Because for either case, only the lower semispherical part of the tip could be in close proximity with the surface, here we have replaced

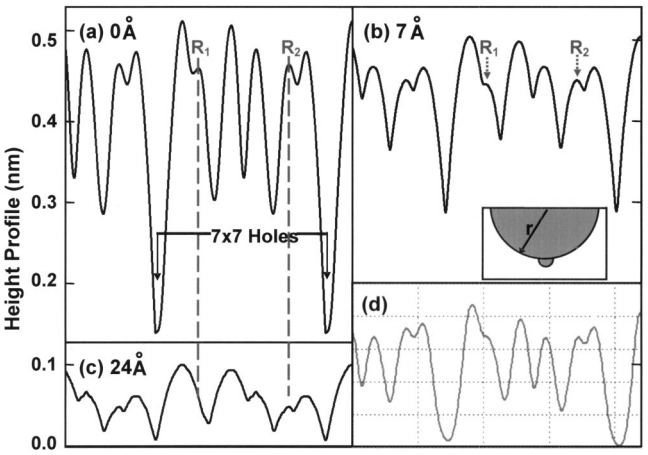

FIG. 3. Line-scans along the diagonal of the 7×7 unit cell for bias voltage=−1.5 V: (a), (b) and (c) are the calculated height profiles with a tip apex radius $r=0.0$, 7.0, and 24.0 Å, respectively, whereas (d) is the experimental profile. Inset shows schematically an STM tip with an adsorbed atomic cluster beneath the apex.

the tip by a sphere of radius r. A small radius of 2 to 3 Å corresponds to case (b) whereas a larger radius corresponds to case (a). To further simplify the calculations, we consider in our simulation only line-scans along the diagonal of the 7×7 unit cell.

Figure 3(a) shows the calculated line-scan at $V_{\text{bias}}=-1.5$ V with an infinitely sharp tip, i.e., $r=0$, as has been done before in most STM image simulations.[20] A sharp tip is also assumed in calculating the images in Figs. 1(a) and 1(b). Next, we trace this $r=0$ curve with a disk of radius r, which is a two-dimensional representation of the three-dimensional sphere, to explore geometric hindrance. It is assumed that at each tip position, tunneling takes place at only one spot on the disk. This is reasonable in most cases because tunneling probability diminishes exponentially with distance. However, there are a few exceptions where the disk is nearly equally distanced from the $r=0$ curve, i.e., at or near the local symmetry points. For simplicity, however, such a tunneling-current doubling effect is ignored in our simulation.

Our results show that for a small disk radius mimicking adsorbed clusters, the line-scan is essentially the same as in Fig. 3(a). Thus, only the larger apex may distort STM images. Figure 3(b) shows the simulated result for $r=7$ Å. At this radius, while none of the main surface topological features have been lost, the overall shape of the line-scan has been significantly modified, noticeably the depth of the profile, and the size of the atoms being noticeably larger than those in Fig. 3(a). Figure 3(c) shows the simulated result for $r=24$ Å. At this radius, the rest atom on the faulted half unit cell has completely vanished. Even for the unfaulted half unit cell, the contrast between the much-more visible rest atom spots and the adatom spots has been greatly reduced. It is thus clear that the attainable size of the tip apex is the crucial factor in imaging the true charge distribution on the 7×7 surfaces. Figure 3(d) shows a corresponding line-scan from our experiment. Despite the simplicity of this model, the calculated result for $r=7$ Å in Fig. 3(b) is in quantitative agreement with experiment. Some of the subtle differences

between Figs. 3(b) and 3(d) could probably even be accounted for by the tunneling-current doubling effect.

In summary, we show STM images which simultaneously and clearly resolve the six rest atoms and twelve adatoms on a Si(111) 7×7 unit cell. Contrary to the widely held belief that rest atoms are invisible to standard STM, they should in fact have almost the same brightness as those of the central adatoms, at least in the unfaulted half unit cells. These results are in agreement with those obtained by first-principles calculations, revealing what should be the "ultimate" STM images for the Si(111)-7×7 surface. This also removes a long-standing misperception that "static" STM calculations (i.e., without the tip-surface interaction and tunneling current effect) can never be quantitative enough to be directly compared to the experimental STM images. The inability of past experiments to observe the rest atoms is also reanalyzed. Our results suggest that a geometric hindrance due to the finite size of the tip apex could be the reason. This prediction should invoke significant research interest in the design and fabrication of the STM tips and their applications in exploring, in general, more detailed physicochemical properties of surface reconstructions and nanostructures.

We thank D.M. Chen and Z.Y. Zhang for helpful suggestions. Work at IOP was supported by National Science Foundation of China with Grant Nos. 90201036, 60228005, and 60125103, National "863" and "973" projects of China, and the Chinese Academy of Sciences. Work at NREL was supported by U.S. DOE/BES and DOE/EERE under Contract No. DE-AC36-99GO10337 and by DOE/NERSC for MPP time.

[1] G. Binnig, H. Rohrer, Ch. Gerber, and E. Weibel, Phys. Rev. Lett. **49**, 57 (1982).
[2] K. Takayanagi, Y. Tanishiro, M. Takahashi, and S. Takahashi, J. Vac. Sci. Technol. A **3**, 1502 (1985).
[3] R. J. Hamers, *Scanning Probe Microscopy and Spectroscopy: Theory, Techniques, and Applications*, edited by D. A. Bonnell (Wiley, New York, 2000).
[4] Z. Y. Zhang and M. G. Lagally, Science **276**, 377 (1997).
[5] G. Binnig, H. Rohrer, Ch. Gerber, and E. Weibel, Phys. Rev. Lett. **50**, 120 (1983).
[6] R. S. Becker, B. S. Swartzentruber, J. S. Vickers, and T. Klitsner, Phys. Rev. B **39**, 1633 (1989).
[7] R. J. Hamers, R. M. Tromp, and J. E. Demuth, Phys. Rev. Lett. **56**, 1972 (1986).
[8] Ph. Avouris and R. Wolkow, Phys. Rev. B **39**, 5091 (1989).
[9] R. Wiesendanger, *Scanning Probe Microscopy and Spectroscopy: Methods and Applications* (Cambridge University Press, Cambridge, England, 1994).
[10] M. A. Lantz, H. J. Hug, P. J. A. van Schendel, R. Hoffmann, S. Martin, A. Baratoff, A. Abdurixit, H.-J. Güntherodt, and Ch. Gerber, Phys. Rev. Lett. **84**, 2642 (2000).
[11] P. Sutter, P. Zahl, E. Sutter, and J. E. Bernard, Phys. Rev. Lett. **90**, 166101 (2003).
[12] P. M. Albrecht and J. W. Lyding, Appl. Phys. Lett. **83**, 5029 (2003).
[13] J. Feng *et al.* (unpublished).
[14] W. Kohn and L. J. Sham, Phys. Rev. **140**, A1133 (1965).
[15] G. Kresse and J. Furthmüller, Comput. Mater. Sci. **6**, 15 (1996).
[16] D. Vanderbilt, Phys. Rev. B **41**, 7892 (1990).
[17] Y. P. Zhang, L. Yan, S. S. Xie, S. J. Pang, and H. J. Gao, Appl. Phys. Lett. **79**, 3317 (2001).
[18] Q. J. Gu, N. Liu, W. B. Zhao, Z. L. Ma, Z. Q. Xue, and S. J. Pang, Appl. Phys. Lett. **66**, 1747 (1995).
[19] S. B. Zhang, M. L. Cohen, and S. G. Louie, Phys. Rev. B **34**, 768 (1986).
[20] J. Tersoff and D. R. Hamann, Phys. Rev. B **31**, 805 (1985).